PHILOSOPHICAL TRANSACTIONS OF THE ROYAL SOCIETY A MATHEMATICAL, PHYSICAL & ENGINEERING SCIENCES

Defect-induced spin disorder and magnetoresistance in single-crystal and polycrystal rare-earth manganite thin films

J. E. Evetts, M. G. Blamire, N. D. Mathur, S. P. Isaac, B.-S. Teo, L. F. Cohen and J. L. Macmanus-Driscoll

Phil. Trans. R. Soc. Lond. A 1998 **356**, 1593-1615
doi: 10.1098/rsta.1998.0237

The Royal Society

Defect-induced spin disorder and magnetoresistance in single-crystal and polycrystal rare-earth manganite thin films

By J. E. Evetts[1], M. G. Blamire[1], N. D. Mathur[1], S. P. Isaac[1], B.-S. Teo[1], L. F. Cohen[2] and J. L. MacManus-Driscoll[3]

[1]*Department of Materials Science, University of Cambridge, Pembroke Street, Cambridge CB2 3QZ, UK*

[2]*Blackett Laboratory, Imperial College of Science, Technology and Medicine, Prince Consort Road, London SW7 2AZ, UK*

[3]*Department of Materials, Imperial College of Science, Technology and Medicine, Prince Consort Road, London SW7 2AZ, UK*

Although theoretical understanding of doped mixed-valence manganites that exhibit colossal magnetoresistance (CMR) is still incomplete, the general observation of a systematic correlation at a given temperature between the magnetization and resistance both above and below the Curie temperature T_C can provide a phenomenological basis for describing the magnetotransport response of defective or magnetically inhomogeneous materials. Defect-related changes in the local magnetization correspond to changes in spin disorder that link to the resistivity through one of several possible spin-dependent transport effects. The different sources and types of defect-induced spin disorder are discussed and an assessment made of transport phenomena that contribute to the magnetoresistive response. Recent measurements of the magnetoresistance of artificial grain boundaries in thin-film bicrystals suggest that spin-polarized tunnelling and spin scattering at interfaces play a relatively minor role, the dominant low-field contribution to magnetoresistance coming from the mesoscale response of magnetic inhomogeneity induced by the grain boundary. The consequence of this finding for other sources of heterogeneity is discussed and the implications for CMR devices and applications are assessed.

Keywords: magnetoresistance; grain boundary; manganite; perovskite materials; spin disorder

1. Introduction

Despite major efforts worldwide there is still no general agreement on a microscopic description of the magnetotransport properties of doped mixed-valence manganites that exhibit colossal magnetoresistance (CMR) in an applied field (Inoue, this volume; Long, this volume; Millis, this volume). Without such a microscopic framework the prospect for a quantitative treatment of defect-induced magnetoresistance in polycrystalline materials and device structures might seem bleak. However, the fact that the same characteristic colossal magnetoresistive behaviour is also observed in other classes of material that differ remarkably from the manganites both structurally and electronically suggests that all models for CMR may not need to be

material specific. Thus the pyrochlores (e.g. $(Tl,Sc)_2Mn_2O_7$) do not exhibit heterovalency and, in contrast to the manganites, have distinct magnetic and electronic sublattices with metallic behaviour for temperatures above the Curie temperature. Furthermore the spinel $(Fe,Cu)Cr_2S_4$ has no manganese, no oxygen and no heterovalency. However, since all these materials display a fairly general scaling of resistivity with magnetization we propose in what follows that, in defective materials, changes in magnetoresistance can usefully be treated phenomenologically in terms of changes in local magnetic order. There is a broad parallel with the remarkable power of the phenomenological Ginzburg–Landau theory in the treatment of the properties of disparate classes of superconductor with radically different microscopic descriptions.

The scaling of resistivity with magnetization, $R(M)$, appears to be systematic and widespread, particularly when data in the literature are evaluated to take account of the fact that it is the local spin disorder within the mesostructure in inhomogeneous systems that determines the overall resistance. The local spin disorder is not necessarily equal to the mean magnetic moment averaged over the sample. Scaling varies from quadratic for M much less than the saturation magnetization, M_s,

$$R = R_0(1 - \beta(M/M_s)^2), \quad M < 0.3M_s, \tag{1.1}$$

to exponential at higher M (Hundley *et al.* 1995; O'Donnell *et al.* 1997). Spin disorder is therefore the primary factor determining changes in resistance with applied field, the different mechanisms will be discussed in § 3. Factors such as electronic bandwidth and bond angle have influence through β, M_s and R_0. In the next section the main features of defectiveness in doped manganites are discussed in relation to these factors, and the issue of the separation of intrinsic and extrinsic magnetoresistive behaviour is addressed.

2. Defectiveness in doped manganites

The doping, stoichiometry, disorder, strain and superlattice structure collectively determine the properties of a CMR manganite. In such a complex situation there is some attraction in attempting to use 'averaged' measures of structure such as valency, tolerance factor, Mn–O distance or Mn–O–Mn bond angle to explain trends in the Curie temperature, T_C, and the magnetoresistance of single crystal material. Although there are many examples demonstrating apparently systematic trends (e.g. bond angle in Fontcuberta *et al.* (1996)), there is also clear evidence that these 'averaged' quantities mask a complex mesostructure arising from the statistical randomness of doping disorder. By appropriate choice of composition it is possible to hold an 'averaged' quantity constant in an alloy series whilst varying significantly the material properties. This is illustrated by the work of Sun *et al.* (1997) who vary the local lattice distortion at constant tolerance factor $t = 0.91137$ in $La_{2/3-x}R_xCa_{1/3}MnO_3$ by suitably adjusting the concentration x of the rare earth R. Thus despite a constant average strain, T_C ranges from 75 to 200 K. Since microstructural defects such as dislocations or grain boundaries severely disrupt the local structure it is therefore likely that T_C will also vary relatively locally in the vicinity of defects.

Further complexity is introduced by the micromagnetic structure which leads to spatial variation of M. Examples are local magnetic anisotropy fluctuations, internal demagnetization due to inhomogeneity and of course domain walls themselves. Although the micromagnetic structure is closely tied to local structure the material can additionally exhibit non-equilibrium magnetic response and hysteresis.

(*a*) *Grain boundary structure and physical characteristics*

Recently there has been considerable interest in the structure and properties of grain boundaries in oxide ceramics (Chisholm & Pennycook 1991; Hilgenkamp *et al*. 1996; Froehlich *et al*. 1997). Although the detailed treatment of low- and high-angle boundaries is quite different, grain boundaries (GB) are generally expected to have associated stress fields and stoichiometry variations as well as electronic characteristics such as local band bending. Chisholm & Pennycook (1991) have calculated the strain distribution at a low-angle tilt boundary, demonstrating that the 1% strain contour extends from the GB at least as far as the characteristic boundary dislocation spacing (4.4 nm for a 5° tilt boundary). While Browning *et al*. (1993) have shown that asymmetric boundaries in a perovskite can exhibit oxygen stoichiometry variations extending several nanometres from the boundary. More recently Mannhart & Hilgenkamp (1998) have argued that band bending and charge-depletion effects determine the transport properties of GBs both in high-temperature superconducting cuprates and in other oxides with similar Thomas–Fermi screening lengths.

In $La_{2/3}Ca_{1/3}MnO_{3-\delta}$ (LCMO) hydrostatic pressure leading to 1% strain results in $\Delta T_C = 10$ K (Laukhin *et al*. 1997) and small changes in δ result in $\Delta T_C = 15$ K (Malde *et al*. 1998). It is very reasonable to expect therefore that locally T_C and $M_s(T)$ vary strongly over several nanometres on each side of a grain boundary, and that the disturbance increases with increasing GB angle.

(*b*) *Other defects, clusters, subgrain boundaries, surfaces*

There are many other less well-defined defects, particularly in thin films, that also lead to significant fluctuations in T_C and as a consequence $M_s(T)$. A very substantial broadening is observed in the magnetoresistive response of thin films with increased characteristic rocking curve widths (figure 1); we attribute this to the MR contribution from the distribution of low-angle subgrain boundaries in such films. Even single-crystal materials display a characteristic low-field magnetoresistive response very close to T_C (O'Donnell *et al*. 1997). This can be explained in terms of a small dispersion of T_C arising from heterogeneity due to local clustering; the effect of such dispersion on the local magnetization dispersion will be maximum at temperatures close to T_C. In these complex mixed-valence compounds there are also likely to be major changes of bonding, symmetry and electronic band structure at surfaces and interfaces with other materials, for instance in heterostructure devices.

3. The characteristics of magnetoresistance in defective material

The intrinsic CMR response of single-crystal manganites and epitaxial thin films with rocking curves of 0.1° or less is quite distinct. The magnetoresistance can be very large but is only observed at temperatures close to T_C, and fields of several tesla are always required for a large MR. Unless there are structural transitions the response is reversible. In contrast 'defective' materials clearly exhibit a significant additional defect-mediated 'extrinsic' MR response. Characteristically the extrinsic MR contribution is observed over the full temperature range $T < T_C$ and there can be a strong MR response at low applied fields; in addition there is a characteristic low-field hysteretic peak structure to the response. In view of the complex heterogeneity existing in these doped manganites even in single-crystal materials one can

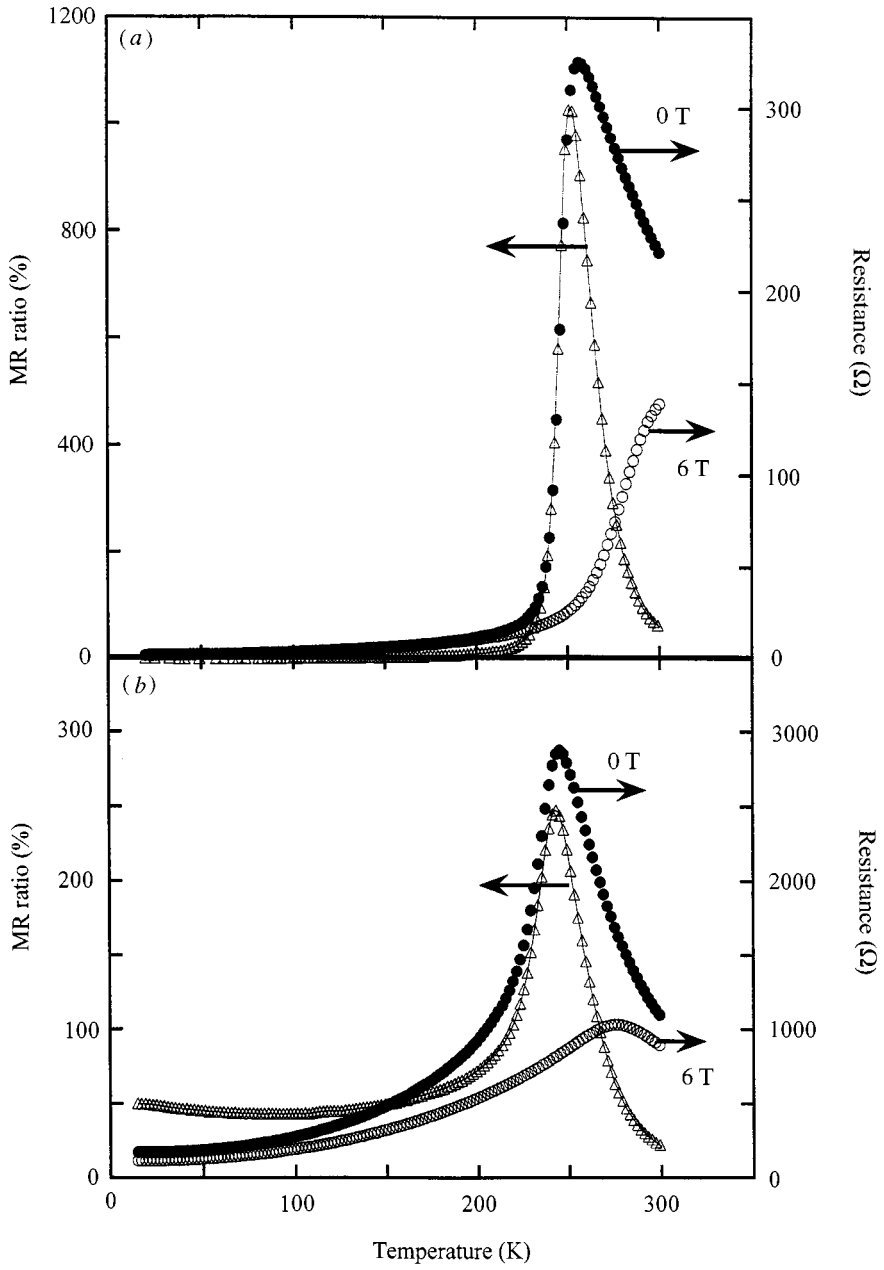

Figure 1. The MR and also resistance in zero field and 6 T for two $La_{0.7}Ca_{0.3}MnO_3$ films with rocking curves of (*a*) 0.1° and (*b*) 1°. The films are of comparable size and shape.

argue over the precise definition of the intrinsic response for these materials; however, there is no disputing the strong extrinsic contribution of various defects, particularly grain boundaries in polycrystalline materials. Viewed phenomenologically the defect structure can either be the direct source of large changes in local spin disorder for small changes in applied field, $\boldsymbol{H}$, or it can be a means of stabilizing a micromagnet-

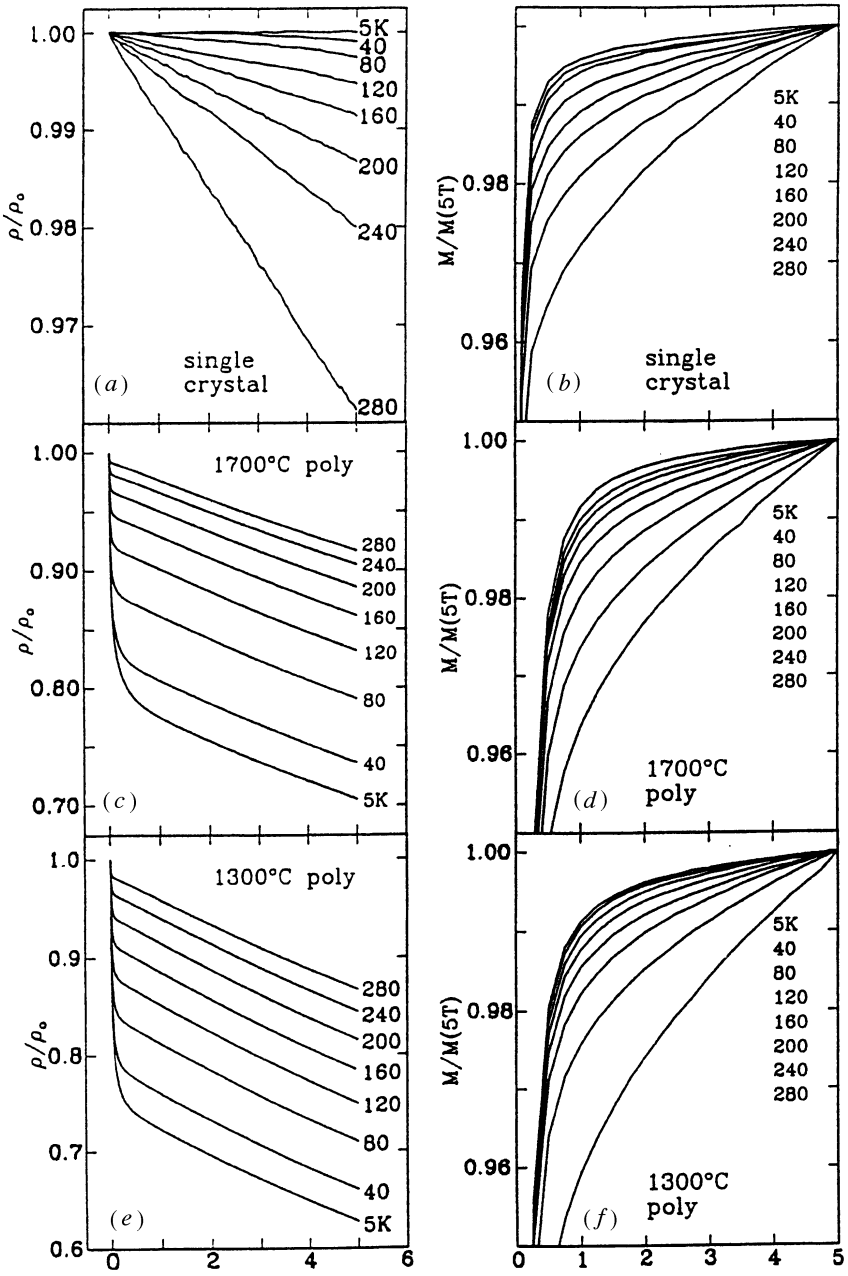

Figure 2. The magnetic-field dependence of the normalized resistance (*a*), (*c*), (*e*) and magnetization (*b*), (*d*), (*f*) of single-crystal and polycrystalline LSMO at various temperatures from 5 to 280 K. (Reproduced from Hwang *et al*. 1996.)

ically induced spin structure (e.g. a domain wall) that responds magnetically in the usual way in an applied field. This distinction is important and will be elaborated further in § 3 *b*.

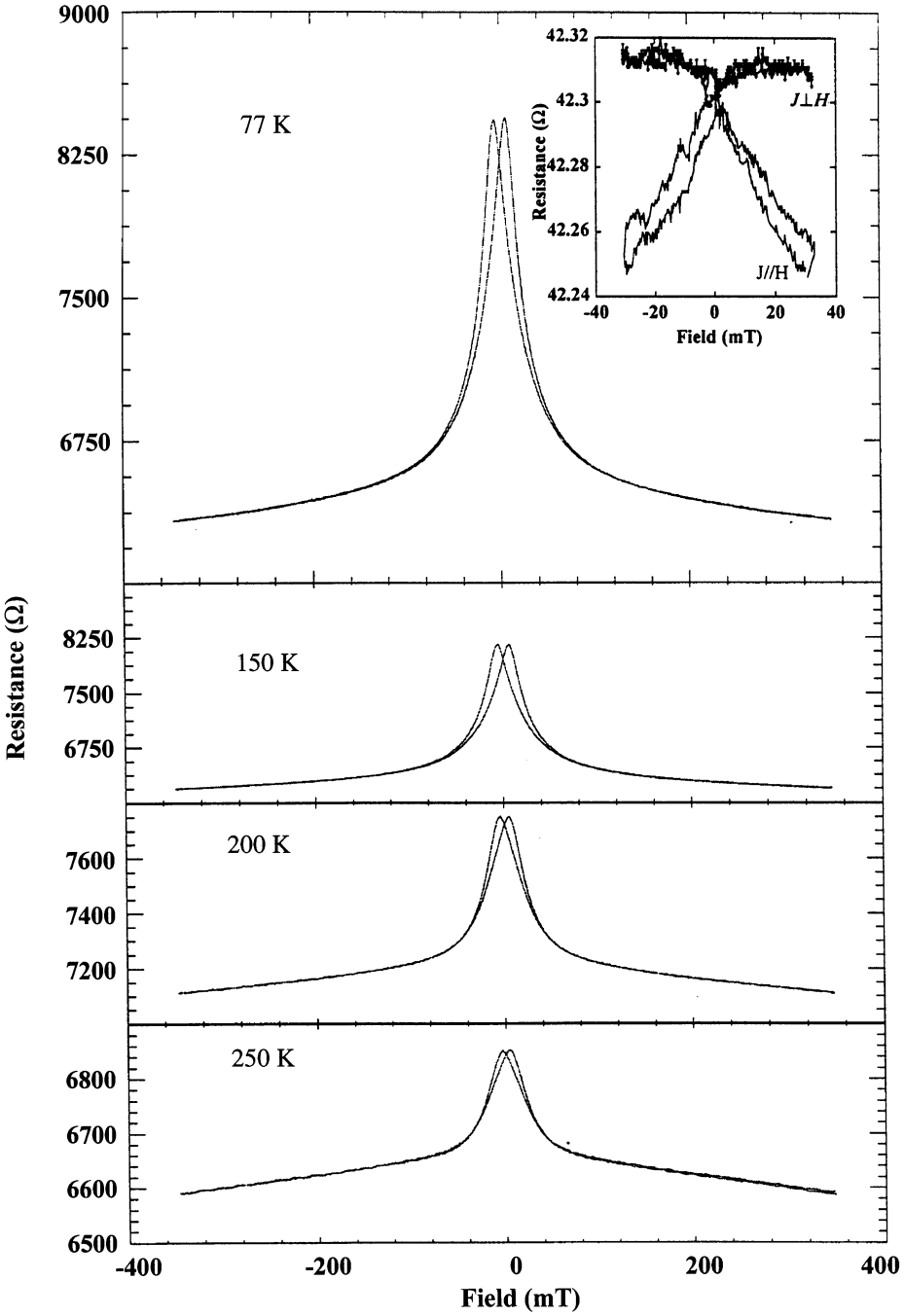

Figure 3. Resistance (R) versus in-plane applied field (H) at a series of temperatures for a LSMO film with a 1° rocking curve width. Inset shows the corresponding $R(H)$ curve with the current parallel and perpendicular to the applied field for a high-quality film with a 0.1° rocking curve width at 77 K.

(*a*) *Polycrystalline materials*

The MR response of polycrystalline materials has been reported in detail for materials with different grain sizes both for bulk materials and thin films. Hwang *et al*. (1996) measure the resistivity $\rho(H,T)$ and $M(H,T)$ for bulk $La_{2/3}Sr_{1/3}MnO_3$ (LSMO) with different characteristic grain sizes. The resistivity at low temperatures is some one to two orders of magnitude greater than that for single-crystal LSMO indicating the dominant contribution of the GB to the resistance in polycrystalline samples. Both polycrystalline samples show a low-field MR as high as 25%, and a characteristic linear variation of resistivity with field at high fields with normalized slope almost independent of temperature (figure 2). Experiments on LCMO thin films with grain sizes 3, 14 and 24 μm yield broadly similar results (Gupta *et al*. 1996). The response is also similar to our observations on epitaxial films with a 1.0° rocking curve (figure 3) confirming that low-angle subgrain boundaries behave in a broadly similar way.

These experiments clearly demonstrate the important role of the GB in manganites but cannot form the basis for a quantitative elucidation of MR transport phenomena at a GB. Measurements on polycrystalline samples can only provide very qualitative information because the MR behaviour is a complex convolution of the response for a distribution of GB angles with different orientations both to the applied field and the measurement current. In the work reported here the MR response of a single GB is isolated and precise measurements are made of the effect of the orientation of the applied field, with the objective of discriminating between different models proposed in the literature for the MR response of polycrystalline rare-earth manganite materials.

(*b*) *Overview of models for magnetoresistance*

The situation is rather open with different models being applied without a full appraisal of the alternatives. In this work the critical features of the different models will be assessed and as far as possible tested in the light of the experimental results obtained. There is some overlap between models but broadly they can be classified as follows.

(i) Spin-polarized tunnelling (SPT) of free carriers through an insulating tunnel barrier; this model is very relevant for heterostructure tunnel devices with the tunnel conductance depending on the polarization direction of the spin system on each side of the boundary. The main features are a resistance, which is independent of T for an 'ideal' barrier, and a constant $R(H)$ at high applied $\boldsymbol{H}$. Temperature dependence can occur if the tunnel barrier is low, in barriers with resonant defect states and in heterogeneous or granular systems.

(ii) Spin-dependent scattering of polarized free carriers is the dominant mechanism describing 'spin valve' processes in metallic multilayers that display giant magnetoresistance (GMR). The model depends on the scattering of conduction electrons by phonons or impurities into the relevant 'spin-polarized' density of available states. Although the carriers may approach 100% polarization in ferromagnetic manganites the analogy with simple GMR systems is incomplete. In addition a model depending on carrier transport with a mean free path determined by electron scattering could only be a realistic approximation for $T \ll T_C$.

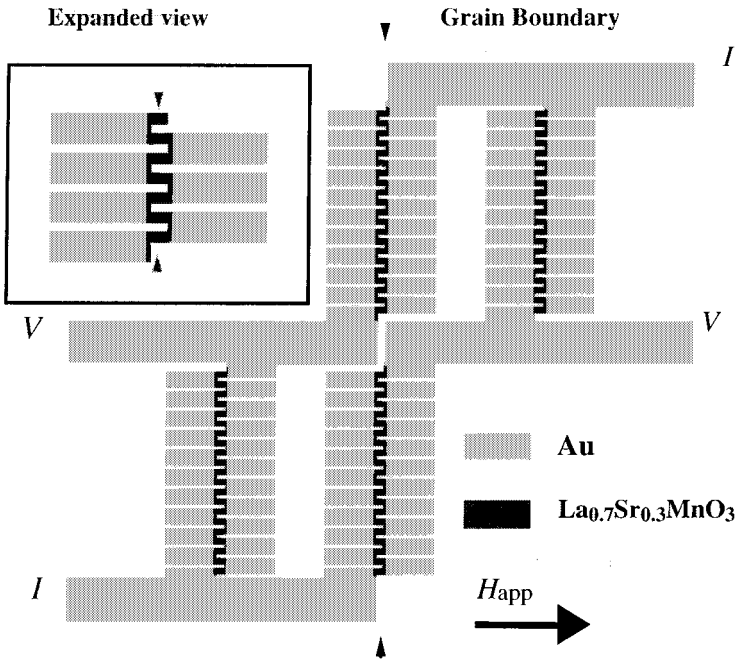

Figure 4. The meander track Wheatstone bridge geometry. Each arm consists of 19 CMR elements, 2 μm wide and 4 μm long. Two of the four arms have artificial grain boundaries induced in the tracks. The arrow indicates the direction of the applied magnetic field, H_{app}.

(iii) Models based on 'activated carrier transport', for example, variable range hopping (VRH) or nearest-neighbour hopping, are generally supported by the temperature dependence of $R(T)$ for $T \geqslant T_{\mathrm{C}}$. Two distinct descriptions of the MR response have to be considered. The first model depends on VRH across a narrow GB when electron hopping is limited because of an abrupt change in the direction of $\boldsymbol{M}$ arising through magnetic anisotropy or a narrow domain wall coincident with the GB. The electron transmission coefficient is the square of the transfer integral which is proportional to $\cos(\frac{1}{2}\theta_{ij})$ where θ_{ij} is the change in direction of $\boldsymbol{M}$ in the characteristic hopping distance. The second model depends on activated carrier transport within the mesoscale region with depressed T_{C} and M_{s} that is associated with a GB. The mesoscale magnetoresistive (MMR) response in an applied field $\boldsymbol{H}$ is determined by changes in the local demagnetization field and the resulting change in the magnetization M_{gb} at the GB. A quantitative treatment of the MMR model is presented in § 5.

4. Isolation of the magnetoresistive behaviour of a single grain boundary

To provide a definitive insight into the role of grain boundaries and to isolate their contribution to the magnetoresistance, we have studied devices patterned from films grown by pulsed-laser deposition on bicrystal substrates. This work was performed in parallel with similar studies on 36.8° bicrystals by the group in Jena (Steenbeck *et al*. 1997).

(*a*) *Device fabrication and testing*

Stimulated by the success of investigations into the nature of grain boundaries deliberately introduced into high-temperature superconductors by growth on bicrystal substrates (Chaudhari *et al*. 1988), we used $SrTiO_3$ bicrystal substrates to induce a single grain boundary in epitaxial thin films of doped lanthanum manganite. To measure the properties of the GB we used a Wheatstone bridge geometry (figure 4) with four identical arms each consisting of 19 $2 \times 4\,\mu m^2$ conductors which were connected by wide gold-coated links. In two of these arms the GB was positioned so as to cut all 19 of these conductors. The bridge geometry effectively subtracts the resistance contribution of the two arms which do not contain the GB from the pair of arms that do and hence the output voltage of the device is a direct measurement of the contribution to the resistance arising from the grain boundary†. These experiments therefore provide a unique probe into the properties of interfaces in these materials.

Epitaxial 200 nm (001) orientated films were grown from a stoichiometric target by pulsed-laser deposition (KrF, $\lambda = 248$ nm) onto $SrTiO_3$ (001) bicrystals at a growth temperature of approximately 800 °C and in an oxygen ambient of 15 Pa. The films were annealed *in situ* at the same temperature in 50 kPa O_2 for 1 h. X-ray diffraction measurements confirmed a single (002) orientation in each film with a typical rocking-curve width of 0.1°. Texture scans also confirmed an in-plane angular misorientation between film halves corresponding to the GB angle of the substrate. The films were patterned by using optical lithography and Ar ion milling at 500 V and 10 mA. To lower the resistance of inactive regions and provide contact pads for Al wire bonding, 60–70 nm of Au was sputter-deposited on each film through a photoresist lift-off mask.

The devices were measured in a variable-temperature liquid-nitrogen cryostat in a magnetic field of up to 300 mT by passing a constant current through each bridge and measuring the voltage across the output terminals. The angle between the sample and the magnetic field could be varied by rotating the sample holder.

We have fabricated samples both with different materials (LSMO and LCMO) and different GB angles (0°, 4°, 24°, 36.8°, 45°). The 0° sample consisted of the same pattern fabricated on a film deposited on a single-crystal substrate.

In addition to the direct measurement of the voltage output of the device, it was also possible to use this geometry to extract the resistance of each arm of the device by measuring the potential difference between the various terminals when a current was passed through the bridge. We were able to test the symmetry of the bridge by subtracting the estimated difference between the two types of arm and comparing this with the direct bridge output—in all cases the difference between the two values was less than 1% which provides a measure of the processing accuracy. A further check on the processing accuracy was the output of the 0° device: asymmetry in the patterning would have resulted in a measurable signal. Two such devices were fabricated which yielded essentially zero output in each case.

† Strictly, the bridge output is half the difference between the resistance of the grain boundary and the equivalent length of undamaged material. However, since the length is currently unknown, and since also below T_C the resistance of the undamaged material is sufficiently low that even if the length extended to hundreds of nanometres the actual resistance difference would still be very close to the resistance of the grain boundary itself, we choose to make this approximation. Above T_C the situation is likely to be different as discussed later.

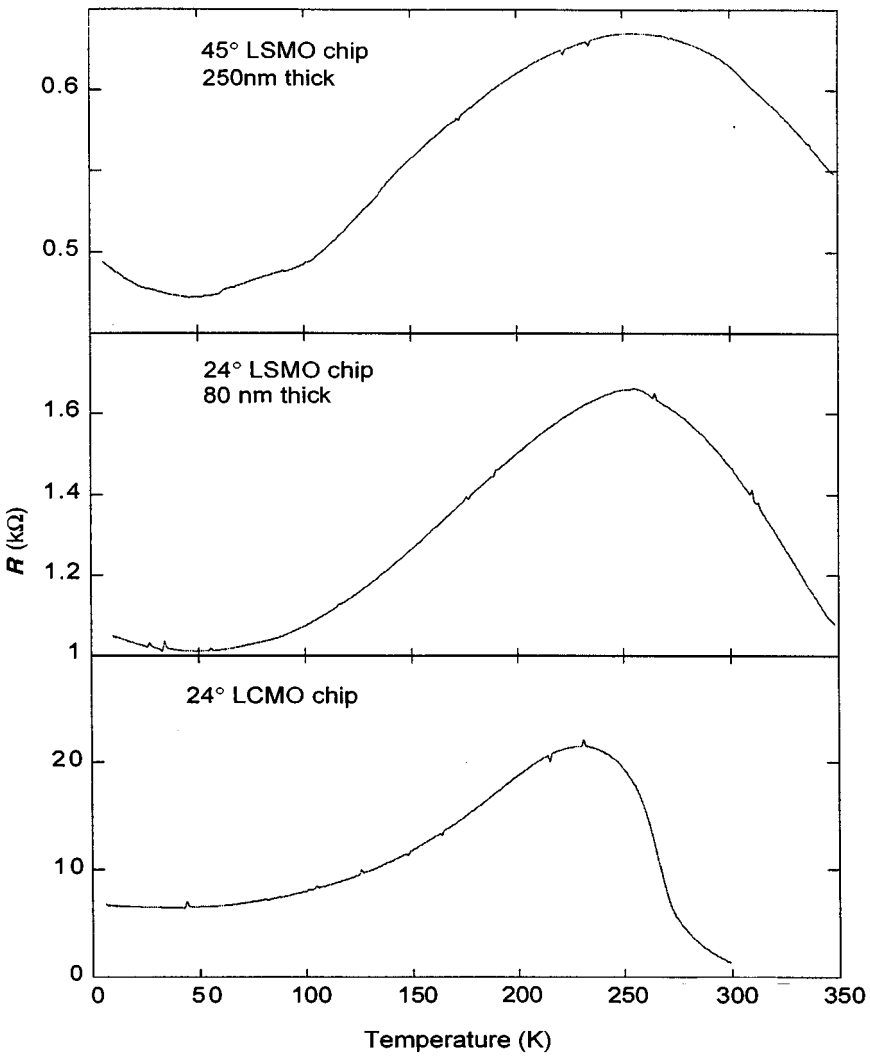

Figure 5. The temperature dependence at zero field of the output resistance of the bridge for the 45° and 24° $La_{0.7}Sr_{0.3}MnO_3$ films and a 24° $La_{0.7}Ca_{0.3}MnO_3$ film.

(*b*) *Experimental results*

Except in the case of the 4° GB, the excess resistance caused by the presence of the grain boundary was substantial, at low temperatures it was greater by at least an order of magnitude than the resistance of the material constituting the remainder of the arms. This resistance becomes larger as the misorientation angle increases. The behaviour of the resistance of the grain boundary in zero applied field as a function of temperature in all cases was very different to the epitaxial film; generally it exhibited a broad maximum well below the Curie temperature of the corresponding epitaxial film (figure 5). In the case of the LCMO device, where we were able to make measurements for $T > T_C$, the output dropped rapidly as the temperature was increased above T_C implying that the resistance of the grain

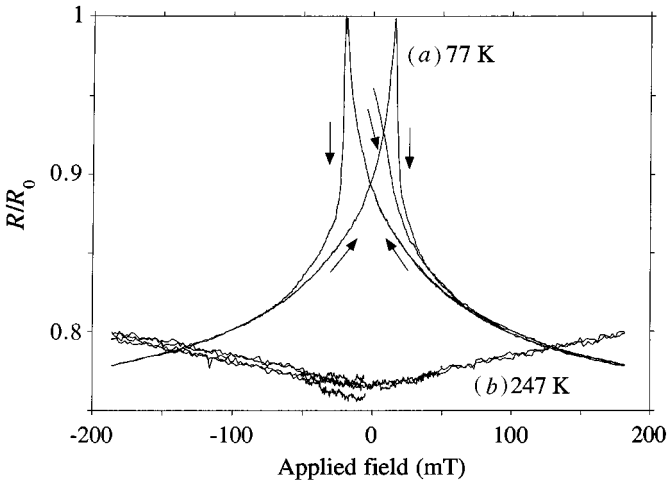

Figure 6. MR as a function of the applied magnetic field for a 24° $La_{0.7}Ca_{0.3}MnO_3$ film at (*a*) 77 K and (*b*) 247 K. For (*b*) the resistance at 180 mT has been used as R_0 and a value of 0.2 has been subtracted from the MR for the purposes of clarity.

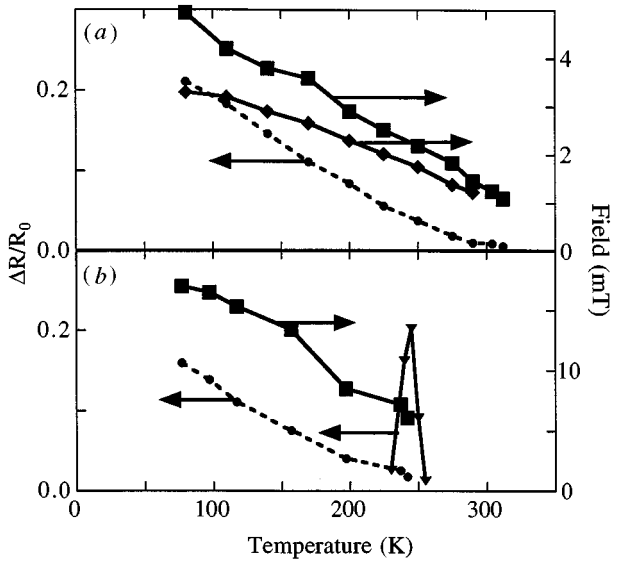

Figure 7. (*a*) Temperature dependence of the MR (•) and the peak resistance field (■) for the 24° $La_{0.7}Sr_{0.3}MnO_3$ grain boundary. The coercive field of a LSMO film grown in the same run is also shown (♦). (*b*) Temperature dependence of the MR and the peak resistance field for a 24° $La_{0.7}Ca_{0.3}MnO_3$ grain boundary. Also shown is the MR of an epitaxial $La_{0.7}Ca_{0.3}MnO_3$ film which is only significant near to the Curie temperature. The line is a guide for the eye.

boundary becomes more comparable to the equivalent length of undamaged material in this temperature range.

A large low field MR was observed in all cases, (except the 0° and 4° device structures), with a hysteretic double-peak structure reminiscent of metallic spin-valve or spin-tunnel devices (figure 6). The exact shape of this hysteresis was strongly sample and temperature dependent, but which ever definition of the low field MR was

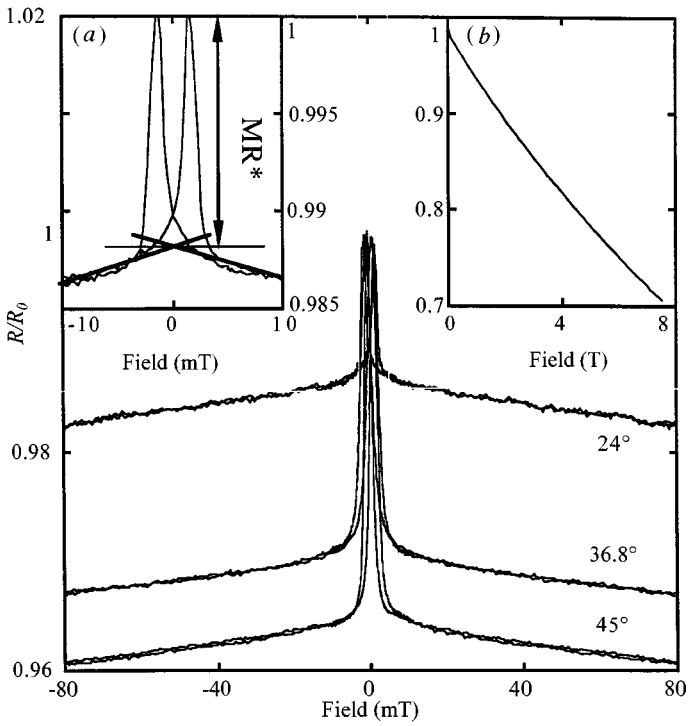

Figure 8. Normalized grain-boundary resistance against the applied field for the 24°, 36.8° and 45° $La_{0.7}Sr_{0.3}MnO_3$ devices measured at room temperature. The inset shows the (*a*) low- and (*b*) high-field dependences for the 24° device. The applied magnetic field is in-plane and perpendicular to the grain boundary.

used, its magnitude increased approximately linearly with decreasing temperature and (at any temperature) increased monotonically with grain boundary angle. In all cases the peak resistances occurred approximately at the coercive field of single crystal films of the same material (figure 7).

At temperatures above T_C for LCMO the hysteresis disappeared, and the grain boundary resistance actually rose with increasing field (figure 6). This behaviour arises in the activated transport regime which dominates above T_C, and would have been masked in measurements of polycrystalline material by the contribution of defect-free material. In our experiment this contribution is balanced out by the bridge structure.

Apart from the hysteretic peak structure, the most striking feature of the data was the remarkable constant high-field slope of the normalized $R(H)$ plots (figure 8). This slope remained almost constant up to fields as high as 7 T (see inset to figure 8). When normalized by the maximum resistance (R_0) this slope was also broadly temperature independent.

The form of the low field $R(H)$ below T_C depends strongly on the angle of the applied field. For fields applied out of the plane of the film demagnetizing effects reduce the effective field to the in-plane component. For fields applied in the plane of the film, the largest effects were observed when the field and current in each link were parallel. Figure 9 shows room temperature $R(H)$ curves for one of the bridge

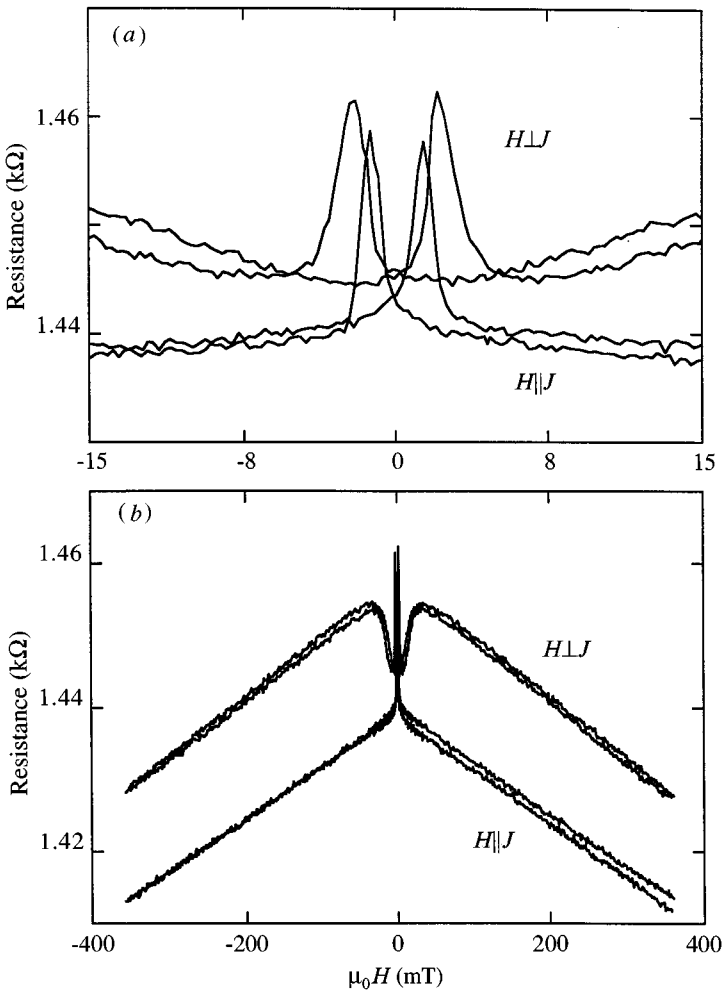

Figure 9. Output resistance of the 24° $La_{0.7}Sr_{0.3}MnO_3$ Wheatstone bridge geometry at 298 K for the two magnetic field directions indicated: (*a*) low-field hysteretic region; (*b*) high-field linear region.

devices with the applied magnetic field $\boldsymbol{H}$ in the plane of the film, and either normal to the grain boundary and therefore parallel to the current ($\boldsymbol{H}\|\boldsymbol{J}$), or perpendicular to the current ($\boldsymbol{H}\perp\boldsymbol{J}$). As discussed previously, in each of these configurations it is possible to identify both a high-field regime above *ca.* 30 mT in which the resistance (output voltage/current) falls approximately linearly with increasing applied field and does not saturate at high field, and a low-field regime in which the differential resistance is hysteretic and sharply peaked. The ($\boldsymbol{H}\perp\boldsymbol{J}$) configuration shows a constant enhancement in the high-field resistance which again persists to high fields.

5. Mesoscale magnetoresistance and local field enhancement

A common feature of recent reports of a sensitive low-field response in polycrystalline materials (Gupta *et al*. 1996; Hwang *et al*. 1996; Snyder *et al*. 1996; Hwang & Cheong

1997; Ju & Sohn 1997; Shreekala *et al*. 1997), and artificial grain boundaries (Mathur *et al*. 1997; Steenbeck *et al*. 1997) is the combination of hysteretic low-field $R(H)$ peak structures with a very constant high-field slope in $R(H)$. In most cases the normalized gradient $(1/R)\,\mathrm{d}R/\mathrm{d}H$ appears to be largely temperature independent, particularly at low temperatures. To our knowledge, there is currently no explanation for this high-field behaviour. Equally, there is no consistent framework which links the low- and high-field regime.

(*a*) *Alternative models for grain boundary magnetoresistance*

Current models fall into two classes, those that attempt to extend existing models for MR in metallic systems and devices by considering the tunnelling or scattering of relatively free carriers, and those that assume that activated carrier transport is the primary transport process. We consider first models based on the concepts implicit in spin-polarized tunnelling (SPT).

The spin polarization of manganite perovskites appears to approach 100%. Thus SPT in devices with manganite electrodes will result in a large low-field MR (since H_C is comparatively low in all CMR materials). The issue to be addressed is therefore not whether SPT is possible, but whether it is the dominant cause of the MR observed in polycrystalline materials. Several authors (Gupta *et al*. 1996; Hwang *et al*. 1996; Hwang & Cheong 1997) have assumed that it is. We suggest here that SPT (unless it takes a very different form in manganites than in the simple metal systems studied to date) is unable to explain all of the features consistently observed in our experiments or those reported for polycrystalline samples.

Magnetoresistance in ferromagnetic tunnel junctions, which essentially consist of an insulating tunnel barrier sandwiched between two ferromagnetic electrodes, was first observed in Fe–Ge–Fe heterostructures by Julliere (1975) who explained the magnetic-field-dependent tunnelling conductance by a simple model relating the tunnelling probability to the relative orientation of the magnetizations of the ferromagnetic electrodes. In Julliere's model, the MR at zero bias can be calculated from the electron spin polarizations of the ferromagnetic electrodes. In general, the MR of junctions having ferromagnetic metals or alloys as electrodes is predicted to have a magnitude of a few tens of percent; and most cases agree moderately well with Julliere's model. Although no explicit temperature dependence is predicted by the model, in all experimental metallic systems, a slow decrease in MR with increasing temperature is observed (Moodera & Kinder 1996) which is usually explained by a combination of spin-flip scattering and resonant (non-polarization-dependent) parallel tunnelling pathways. Typically the MR of simple metal junctions at 4.2 K is of the order of 50% higher than the room temperature value.

$R(H)$ plots for metal tunnel junctions exhibit a hysteretic peak structure which can be similar to those observed for the polycrystalline manganites. However, there is a clear difference in the behaviour at high fields. For simple tunnel junctions the resistance saturates rapidly once the field exceeds the coercive field of the electrodes; in other words once the magnetization is parallel in the two electrodes there are no further possible changes which affect the tunnel probability and so the tunnel conductance remains constant.

The conductance of a simple tunnel junction (at any applied field) depends only on the magnitude of the tunnelling probability. This should be temperature inde-

pendent for an insulating barrier whose height considerably exceeds kT. There are several possibilities which can result in a temperature dependence: the freezing out of resonant tunnelling pathways in imperfect barriers, a low barrier height which results in thermally activated carriers having an enhanced tunnel probability, or (in the case of very low barrier heights) thermionic emission of carriers over the barriers. Hwang *et al*. (1996) cite the work of Helman & Abelas (1976) on SPT in nanoscale granular nickel and suggest temperature-dependent SPT can arise in manganites through magnetic coupling effects across the barrier. In all of these cases, however, one expects a monotonic decrease in barrier conductance as the temperature is reduced. It is therefore difficult to model the complex, but consistent, temperature dependence of the zero-field resistance that we have measured in our devices. A further factor which we believe it is difficult to explain on the basis of SPT is the strong dependence of $R(H)$ on the in-plane angle of the applied field at intermediate and high fields.

To explain the experimental MR results for the manganites we therefore require a model which is capable of simultaneously explaining both the hysteretic low-field response (and its temperature dependence), the high-field linear background, and the temperature dependence of the grain-boundary resistance. Although models that start within the activated carrier transport regime cannot draw on experience with metallic systems, they have the advantage of being able to use concepts closer to the accepted microscopic configuration of the doped manganites. The simplest model for MR at a GB depends on the variation of the transfer integral $T_{ij} = t_1 \cos(\frac{1}{2}\theta_{ij})$ for an electron crossing the GB when there is an abrupt change in the angle θ_{ij} of the $\boldsymbol{M}$ at the boundary. The approach is attractive because within a defect-free manganite the resistance $R \sim R_0 \exp(-\Gamma_{ij})$, where $\Gamma_{ij} = (T_{ij})^2$ is the electron transmission coefficient, and since $M(H,T) \sim \langle \cos(\frac{1}{2}\theta_{ij}) \rangle$ within a disordered spin system one can expect the resistance to scale as $R \sim R_0 \exp(-\gamma M^2)$ as observed generally in these CMR materials. The problem with the simple picture of an abrupt change in direction for $\boldsymbol{M}$ at a GB is that $R(H)$ due to the GB is constant at high fields. Furthermore the observed GB resistance is too high to be described by an abrupt (narrow) GB. We therefore introduce a model that depends on activated carrier transport within a defective region adjacent to a GB. The MR is in effect the CMR response of a highly disordered mesoscale region with a depressed T_C and magnetization, M_{gb}.

(*b*) *Basis of the model*

We have identified three significant factors which we believe govern the grain boundary CMR response in doped manganite perovskites and which are therefore fundamental to any applicable model.

(i) *Strain fields*

It is well known that strain dramatically effects the magnetic (and therefore transport) properties (Gupta *et al*. 1996; Laukhin *et al*. 1998; Hwang & Cheong 1997; Ju & Sohn 1997) of the CMR manganites and hence we can conclude from the discussion of § 2 *a* that a region of substantially suppressed magnetic order will exist at any grain boundary, with the degree of suppression being a strong function of the grain-boundary angle. Although this idea can also be invoked for SPT, it should

be noted that there is no suggestion that this suppressed region need behave as an insulator—indeed work on high-temperature perovskite superconductors has indicated that the changes in electrical resistivity are modest (Mannhart & Hilgenkamp 1998) and all effects which lead to the creation of Josephson junctions at grain boundaries relate to the suppression of the superconducting critical temperature to create a superconductor–normal–superconductor junction.

(ii) *Magnetic environment*

It follows that if a grain boundary is a mesoscale region of depressed magnetic order then since $\boldsymbol{B}_\perp = \mu_0(\boldsymbol{H} + \boldsymbol{M})_\perp$ and $\boldsymbol{H}_\parallel$ are continuous at an interface the adjacent intragranular regions will have a strong influence on the local field $\boldsymbol{H}_{\rm gb}$. In addition, it is likely that exchange coupling between the intragranular material and the grain-boundary region will enhance the magnetic order which would be present in the strained region in isolation.

(iii) *Orientation of external field*

The orientation of the applied magnetic field H with respect to the grain boundary has a large effect on the experimental results and must be accommodated. The degree of continuity of magnetic flux (see § 5 *b* (ii)) will certainly depend on the angle of the applied field, and so can affect local magnetic order and hence the transport behaviour.

We therefore propose that we are dealing with a mesoscale phenomenon for which a mesoscale solution is required. Accordingly, we present a model which is consistent with measurements of an artificial grain boundary that show an orientation dependence on applied field direction not previously seen.

(*c*) *The mesoscopic magnetoresistance (MMR) model*

To account for interfacial strain at the grain boundary we assume that there is a region of depressed magnetic order near the artificial grain boundary. The resistivity $R_{\rm gb}$ of this region is represented by the device output R and so can be measured directly. We assume that $R_{\rm gb}$ is determined by the magnetization $M_{\rm gb}$ within the region according to the same relation for bulk CMR material whether above or below $T_{\rm C}$ (Hundley *et al*. 1995; Fontcuberta *et al*. 1996; O'Donnell *et al*. 1996, 1997; Shimakawa *et al*. 1996). Thus

$$R_{\rm gb} = R_0 \exp[-\gamma M_{\rm gb}^2], \tag{5.1}$$

where $\gamma \propto M_{\rm s}^{-2}$, $M_{\rm s}$ is the fully spin aligned saturation magnetization of the material and R_0 is the average grain-boundary resistivity when $M_{\rm gb} = 0$.

To quantify $M_{\rm gb}$ we invoke magnetic continuity discussed in § 5 *b* (ii). The continuity of the perpendicular component of the magnetic flux density between the strained grain-boundary region and the intragranular material ensures that the reduction in magnetization in the grain boundary is compensated by an increase in local field $H_{\rm gb}$. Adopting the terminology of the magnetic device community, the intragranular material can be said to constitute a 'soft adjacent layer' or SAL. The increased local field in the grain-boundary region arises from contributions due to the local magnetization everywhere in the intragranular regions via an integral expression. It

therefore depends on the orientation of the applied field $\boldsymbol{H}$, which thus incorporates into the analysis our third significant factor.

We represent the average SAL field within the grain boundary region by the expression fM_{g}, whose magnitude is some fraction f of the magnitude of the magnetization $\mu_0 M_{\mathrm{g}} \approx \mu_0 M_{\mathrm{s}} \sim 560\,\mathrm{mT}$ in the intragranular regions. For field magnitudes well in excess of the coercive field we assume that each of these regions is single domain and therefore f depends only on the direction of $\boldsymbol{H}$.

We write M_{gb} as a sum of the reduced spontaneous grain boundary magnetization M_0 and an isotropic linear response term χ_{gb} which describes the effect of both the externally applied field $\boldsymbol{H}$ and the SAL field fM_{g}:

$$M_{\mathrm{gb}} = M_0 + \chi_{\mathrm{gb}}(fM_{\mathrm{g}} + H), \tag{5.2}$$

where χ_{gb} is small. The finite value of M_0 results from the (weakened) local ferromagnetic interactions, and possibly also from exchange coupling with the adjacent intragranular regions.

Substituting for M_{gb} in (5.1) using (5.2), neglecting terms which are quadratic in χ_{gb} and expanding the exponential we obtain

$$R_{\mathrm{gb}} \approx [1 - \gamma\{(M_0^2 + 2M_0\chi_{\mathrm{gb}} fM_{\mathrm{g}}) + (2M_0\chi_{\mathrm{gb}})H\}], \tag{5.3}$$

which describes the dependence of the grain-boundary resistance on the magnitude and angle of the applied field. Any temperature dependence of the resistance is included in the terms M_0, M_{s} and χ_{gb}.

Having established (5.3) we can use it to describe the various aspects of the experimental results in the high-, intermediate- and low-field regimes, respectively.

(i) *High-field regime: constant slope*

Magnetization measurements on epitaxial LSMO thin films made with a vibrating sample magnetometer revealed that M_{g} is approximately independent of field for $H > H_k$, where H_k is the magnetic anisotropy field for the device structure. Therefore only the final term within the brackets in (5.3) is field dependent in the high-field limit with the result that (neglecting terms quadratic in χ_{gb}) the normalized device output is linear in the high-field regime as observed:

$$\frac{\mathrm{d}R_{\mathrm{gb}}}{R_0\,\mathrm{d}H} \approx -2\gamma\chi_{\mathrm{gb}}M_0. \tag{5.4}$$

Expression (5.4) for the slope is orientation independent since f does not appear, and this is consistent with our findings (figure 9).

The enhancement in the high-field resistance observed in figure 9 when $\boldsymbol{H}\perp\boldsymbol{J}$ is a consequence of M_{g} being parallel to the grain boundary rather than perpendicular to it, such that f is reduced. From (5.3) we can write the difference between the high-field linear response seen in figure 9 when $\boldsymbol{H}\|\boldsymbol{J}$ and $\boldsymbol{H}\perp\boldsymbol{J}$ as $2\gamma\chi_{\mathrm{gb}}\Delta f M_0 M_{\mathrm{g}} R_0$, where Δf represents the difference between f in the two geometries. Using (5.3) and our experimental data we find $\Delta f \sim 0.4$, which is consistent with significant grain-boundary deviations.

(ii) *Intermediate-field response*

For intermediate fields when $H_{\mathrm{C}} < H < H_k$ the MR response shows a complex dependence on field and angle. In this regime the shape anisotropy of the long thin

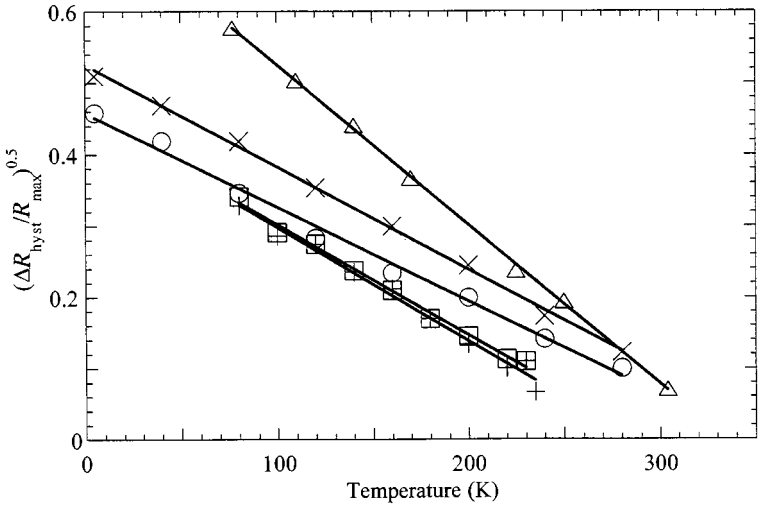

Figure 10. The temperature dependence of $(\Delta R_{\rm hyst}/R_0)^{0.5}(M_0)$ for several grain boundary structures. +, □, LCMO bicrystal device measured at 100 and 400 mT, respectively; △, LSMO bicrystal device; ○, ×, polycrystalline samples (data from Hwang *et al*. 1996).

tracks of the device structure begins to determine the direction of $M_{\rm g}$. As $\boldsymbol{H}$ is reduced the demagnetizing fields progressively overcome the applied field and $M_{\rm g}$ rotates to the 'easy' direction for the device. This can be seen in figure 9 where the curve for $\boldsymbol{H}\perp\boldsymbol{J}$ drops down to join the curve for $\boldsymbol{H}\|\boldsymbol{J}$ as the field is reduced. Based on the position of the shoulder in the $\boldsymbol{H}\perp\boldsymbol{J}$ curve it is possible to estimate the anisotropy field $H_{\rm shape}$ of the uninterrupted film away from the grain boundary to be $\mu_0 H_{\rm shape} \sim 30$ mT.

(iii) *Low-field hysteresis*

In the low-field regime, we use (5.3) to yield an expression for $\Delta R_{\rm hyst}$ by assuming that $M_0 = 0$ at $H_{\rm C}$. This, for example, would be a natural consequence of the SAL electrodes exchange coupling strongly to the grain boundary region. It follows that

$$\frac{\Delta R_{\rm hyst}}{R_0} \approx \gamma[M_0^2 + 2M_0\chi_{\rm gb} f M_{\rm g}] \approx \gamma M_0^2. \tag{5.5}$$

Here we assume that $\chi_{\rm gb}$ is much less than unity which is likely to be valid in all temperature ranges and is certainly true above $T_{\rm C}$ where $\chi_{\rm gb}$ is simply equal to the zero field susceptibility.

To investigate the temperature dependence of M_0 we plot in figure 10 the temperature dependence of $(\Delta R_{\rm hyst}/R_0)^{1/2}$ for one of our LSMO devices alongside similar data from Hwang *et al*. (1996). The origin of the extreme linearity of the plots for this parameter versus temperature obtained from both bulk polycrystalline material and bicrystal thin-film devices is unknown, but is clearly worthy of further investigation.

Given that we observe the high-field normalized gradient of the device output to be highly temperature independent, the fall in M_0 with increasing temperature seen in figure 10 suggests via equation (5.4) that $\chi_{\rm gb}$ increases with increasing temperature. It is important to bear in mind that $\chi_{\rm gb}$ represents the differential high-field susceptibility of the material (5.2) which must tend to zero as M_0 tends to $M_{\rm s}$.

It is beyond the scope of this model to account for the precise temperature dependences of M_0 and χ_{gb}, but the suggested trends are consistent with the postulated depressed ferromagnetic order. A full treatment would need to consider the inhomogeneity which arises due to the presence of complex strain fields near perovskite grain boundaries (Chisholm & Pennycook 1991).

6. Summary and discussion

We have presented a phenomenological model which can self-consistently link the contribution of grain boundaries to the high- and low-field transport behaviour of perovskite CMR materials. In so doing we provide an explanation for the striking high-field linear response. Our model depends on analysis of the micromagnetic response of the grain boundary viewed as a mesoscale magnetic artefact and is based on three physical factors: strain near interfaces, the effect on a strained interface of adjacent magnetized regions and the variation of the micromagnetic local fields with applied field orientation. Evidence for the characteristic angular variation is clear in our measurements on an isolated grain boundary but would be masked in experiments on polycrystalline films.

A reduced spontaneous magnetization in the interfacial region suggests that antiferromagnetic interactions start to dominate in strained perovskite CMR materials of increased resistance. This is consistent with high-field magnetization measurements we have made on LSMO films of differing quality, but our findings are at variance with the findings of Gupta *et al*. (1996). In common with O'Donnell *et al*. (1997) our highly epitaxial films (0.1° rocking curve width) show a small hysteretic low-field MR response near T_C (inset of figure 3) which we understand within the framework of our model to arise because of magnetic inhomogeneity in the subgrain boundaries, direct experimental evidence of which has been observed by Domínguez *et al*. (1996) in high-quality films near T_C. Since there are complex strain fields near perovskite interfaces (Chisholm & Pennycook 1991), any definition of the 'width' of the grain boundary region is somewhat elastic, but given a resistance multiplied by a cross-sectional area product of *ca*. $6 \times 10^{-11}\,\Omega\,m^2$ for the grain-boundary contribution to each track and assuming a maximum resistivity of $10^{-2}\,\Omega\,m$ (Gupta *et al*. 1996) places a lower bound on the extent of the disordered region at 6 nm, which is plausible in light of the TEM evidence presented in Gupta *et al*. (1996).

7. Conclusions and outlook for technical implementation

Measurements on isolated grain boundaries with different grain-boundary angles have established unequivocally that such defects contribute a strong 'extrinsic' magnetoresistive component to the underlying intrinsic CMR response. An assessment has been made of the applicability of different current models for the MR contribution of a grain boundary. In general it is concluded that models based on 'activated carrier transport' are more likely to find quantitative application in these materials. A new model is presented which takes account of the local micromagnetic response of a defect and postulates a mesoscale magnetic region with magnetic properties altered from those of the bulk. The model is phenomenological and exploits the observation of a very general scaling of the resistivity of CMR materials with magnetization; the model therefore has wide applicability and may also apply to other classes of

materials displaying CMR. The mesoscale magnetoresistance (MMR) is evaluated quantitatively and is shown to be able to account for much of the experimental behaviour. Although the model cannot at this stage be said to be the only model that indisputably provides a description of the MR contribution of grain boundaries in doped manganites, it clearly has validity as a model that relates for the first time the micromagnetic MR response of a material to the heterogeneity of a mesoscale defect structure. Even if the MMR proves not to be the dominant mechanism in the case of grain boundaries there are other model systems where it can clearly be applied. Other defect types and also areas of controlled damage, for instance ion beam damage, can have the required geometry to contribute to the magnetoresistance in this way.

There is clearly scope for the design of manganite-based devices with tailored low-field MR response. In designing such devices it is important to understand and control both the defect structure and the micromagnetic behaviour of the structures. At present the low-field MR at room temperature is limited to about 3% (Isaac *et al.* 1998); however, optimization of the low field MR can be explored: (i) by adjusting the properties of the damaged region to give maximum response at the operating temperature; and (ii) by careful design of the micromagnetic response to maximize the magnetic flux density at the interface to the defective region. Although the low-field hysteresis is a problem for many applications it may be possible to exploit a change in Δf to produce an MR response rather than changing the applied field directly.

This work was supported by the Engineering and Physical Sciences Council under the Advanced Magnetics Programme. S.P.I. is grateful to Oxford Instruments plc for support through a CASE studentship.

References

Browning, N. D., Chisholm, M. F., Pennycook, S. J., Norton, D. P. & Lowndes, D. H. 1993 *Physica* C **212**, 185–190.

Chaudhari, P., Mannhart, J., Dimos, D., Tsuei, C. C., Chi, J., Oprysko, M. M. & Scheuermann, M. 1988 *Phys. Rev. Lett.* **60**, 1653–1656.

Chisholm, M. F. & Pennycook, S. J. 1991 *Nature* **351**, 47–49.

Dominguez, M., Lofland, S. E., Bhagat, S. M., Raychaudhuri, A. K., Ju, H. L., Venkatesan, T. & Greene, R. L. 1996 *Solid State Commun.* **97**, 193–196.

Fontcuberta, J., Martínez, B., Seffar, A., Piñol, S., Garcia-Muñoz, J. L. & Obradors, X. 1996 *Phys. Rev. Lett.* **76**, 1122.

Froehlich, O. M., Richter, P., Beck, A., Gross, R. & Koren, G. 1997 *J. Low Temp. Phys.* **106**, 243–248.

Gupta, A., Gong, G. Q., Xiao, G., Duncombe, P. R., Lecoeur, P., Trouilloud, P., Wang, Y. Y., Dravid, V. P. & Sun, J. Z. 1996 *Phys. Rev.* B **54**, 15 629–15 632.

Helman, J. S. & Abeles, B. 1976 *Phys. Rev. Lett.* **37**, 1429.

Hilgenkamp, H., Mannhart, J. & Mayer, B. 1996 *Phys. Rev.* B **53**, 14 586–14 593.

Hundley, M. F., Awley, M., Heffner, R. H., Ji, Q. X., Neumeier, A., Tesmer, J., Thompson, J. D. & Wu, X. D. 1995 *Appl. Phys. Lett.* **67**, 860.

Hwang, H. Y. & Cheong, S. W. 1997 *Nature* **389**, 942–944.

Hwang, H. Y., Cheong, S. W., Ong, N. P. & Batlogg, B. 1996 *Phys. Rev. Lett.* **77**, 2041–2044.

Isaac, S. P., Mathur, N. D., Evetts, J. E. & Blamire, M. G. 1998 *Appl. Phys. Lett.* **72**, 2038–2040.

Ju, H. L. & Sohn, H. 1997 *Solid State Commun.* **102**, 463–466.

Julliere, M. 1975 *Phys. Lett.* A **54**, 225.

Laukhin, V., Fontcuberta, J., GarciaMunoz, J. L. & Obradors, X. 1997 *Phys. Rev.* B **56**, 10 009–10 012.

Malde, N., de Silva, P., Hossain, A., Cohen, L. F., Thomas, K. A., MacManus-Driscoll, J. L., Mathur, N. D. & Blamire, M. G. 1998 *Solid State Commun.* **105**, 643–648.

Mannhart, J. & Hilgenkamp, H. 1998 *J. Mater. Sci.* (In the press.)

Mathur, N. D., Isaac, S. P., Burnell, G., Teo, B.-S., Cohen, L. F., MacManus-Driscoll, J. L., Evetts, J. E. & Blamire, M. G. 1997 *Nature* **387**, 266–268.

Moodera, J. S. & Kinder, L. R. 1996 *J. Appl. Phys.* **79**, 4724.

O'Donnell, J., Onellion, M., Rzchowski, M. S., Eckstein, J. N. & Bozovic, I. 1996 *Phys. Rev.* B **54**, 6841.

O'Donnell, J., Onellion, M., Rzchowski, M. S., Eckstein, J. N. & Bozovic, I. 1997 *Phys. Rev.* B **55**, 5873.

Shimakawa, Y., Kubo, Y. & Manako, T. 1996 *Nature* **379**, 53.

Shreekala, R. *et al*. 1997 *Appl. Phys. Lett.* **71**, 282.

Snyder, G. J., Hiskes, R., DiCarolis, S., Beasley, M. R. & Geballe, T. H. 1996 *Phys. Rev.* B **53**, 14 434–14 444.

Steenbeck, K., Eick, T., Kirsch, K., O'Donnell, K. & Steinbeiss, E. 1997 *Appl. Phys. Lett.* **71**, 968.

Sun, J. R., Rao, G. H. & Liang, J. K. 1997 *Appl. Phys. Lett.* **70**, 1900–1902.

Discussion

P. B. Littlewood (*University of Cambridge, UK*). Both Dr Evetts and Dr Fontcuberta suggested that there should be a rather thickish dead layer, or suppressed T_C layer, on the surface. A suppression of T_C of about 10 K seems plausible, but Dr Evetts also then required, for the last part of his model, that the magnetization in that regime is not saturated up to fields of up to 7.5 T. Is this kind of weak suppression correct?

J. E. Evetts. I think Professor Littlewood is right. Given the stress distribution of the grain boundary, we have a spread of T_C, compression, dilation and shear over quite a broad band, all the way down the boundary. There is oxygen depletion as well, depending on where you are on this wavy boundary. This means that we must take averages. There's quite a nice figure here (figure 5) which hasn't been fully interpreted yet, but which gives some suggestion as to what might be happening. We have an LSMO grain boundary in which the actual resistance swings over some sort of broad peak way below T_C, but we still have this drop at low field (which Hwang gets as well, it all fits) which is small at high temperatures and gets much larger at low temperatures. This does imply that there is some sort of feature which is maybe 50 or 100 K below T_C, which could describe the material.

G. A. Gehring (*University of Sheffield, UK*). Why hasn't Dr Evetts considered that the boundary layer could be either antiferromagnetic or a spin-glass? He has a constant susceptibility (at least in mean field) for a perpendicular field, and this would have a constant susceptibility up to a high field.

J. E. Evetts. We did for a long while and have only recently abandoned that, the reason being that it cannot explain the constant slope at high field. You need to get that M_0 term in there in order to get something that is linear in H, which is rather important.

G. A. Gehring. Why doesn't it explain it? The magnetization would continue to cant round in high fields.

J. E. Evetts. If the $\exp(-\gamma M^2)$ term is expanded, it is the M^2 expansion that gives you various powers of H, and you've got to have an H term coming out there to give you the linear term at high fields. The other major thing which doesn't work very well is that it is hard to get the drop at the coercive field to be consistent with the slope of the linear high field regime. I think it's open. If someone could come along with a model where antiferromagnetic materials would fit, perhaps even with a negative Curie–Weiss constant (which we had for some while), then that would be great, but at the moment we are focusing on something with a depressed T_C in the grain boundary.

T. Venkatesan (*University of Maryland, USA*). Looking at the resistance versus field for the case of J perpendicular to H, there is a bump between the low field and high field regimes whereas in the parallel case the curve comes all the way down. Can Dr Evetts explain that?

J. E. Evetts. Yes, that's very easy to explain. Above the anisotropy fields, whatever they are caused by, whether they are intrinsic anisotropy, magnetocrystalline anisotropy or shape anisotropy, all the moments are pretty well parallel and hence perpendicular to the current. Thus there is a difference between the H parallel and H perpendicular geometries. As the field is reduced you get to a point where the shape anisotropy starts to dominate and pulls the magnetization round towards the same sort of orientation as the H parallel to J configuration.

M. Rzchoswki (*University of Wisconsin-Madison, USA*). It seems like Dr Evetts's interpretation depends on the grain boundary material not being dramatically different from the bulk material and showing the same sort of functional dependence of resistivity on magnetization. For a low angle boundary, which can be modelled with dislocations, you might expect that, but at 24 and 36° I would think that the entire cation stoichiometry would be entirely different from the electrode.

J. E. Evetts. Should we really be using $\exp(-M^2)$?

M. Rzchoswki. Perhaps there is an insulating antiferromagnet at the boundary, rather than a ferromagnet with a lower T_C CMR material?

J. E. Evetts. The first point, which I made at some length in § 1 of the paper, is that I think very generally all materials, whether spinels, pyrochlores, however disordered, whatever the doping, very often give $\exp(-M^2)$, and so I think whatever terrible things we do to this boundary we are actually going to have to apply the same phenomenology (that's just an assumption). Now, what Dr Rzchoswki would say is that he does not really like the idea of this boundary surviving with a T_C at all. This is similar to Professor Gehring's suggestion, I think that's probably going a long way and nobody has gone as far as that yet and what I was quite pleased at is that we're coming out with real numbers such as 35 Ω for a 2 μm wide grain boundary in a 200 nm thin film, and if you compare that with this sort of data here for LCMO, as you depress T_C and really distort this material, all you are doing is tracking up a universal master curve. So what we should do is, if we feel we have depressed T_C to 250 or 200, we expect to get this resistivity for the material, and in fact if you take your 35 Ω for our boundary and estimate a width of, say, 2–5 nm, you

come out very nicely in the right sort of range here. So I do believe that this material is still a reasonable manganite with depressed properties of one sort or another. The magnetization curve M_0 does seem to be rather flat, so it could have a sort of spin disorder type character to it. We do have a sort of estimate for M_0, and it does seem to vary in a rather flat way with temperature, which could be significant.

R. Stroud (*Naval Research Laboratory, Washington, USA*). We have done some radiation damage studies where we deliberately add in structural disorder, and we have managed in some slightly oxygen deficient films to create films with both a ferromagnetic transition and an antiferromagnetic transition. I think with the slight amount of disorder, where we are talking about say 2% of the atoms displaced, you can actually create local regions with antiferromagnetic disorder, so I suggest that Dr Evetts should look for it too.

A. J. Millis (*The Johns Hopkins University, USA*). Is it possible to do microscopy, for example, to find out what exactly is at the grain boundary? Dr Evetts showed us pictures (see Chisholm & Pennycook 1991) of calculated strain fields (obviously strain is important), but there must also be local things, so how should I really think of it?

J. E. Evetts. There's been a lot of work on the YBCO boundaries, which is a layered perovskite and so liable to be slightly different, there is real disorder spreading far less distance than the strain. I know of one micrograph, in Gupta *et al*. (1996), but there are very few on the ground, and it's one of the things which we intend to do. From this particular grain boundary we will cut a section with a focused ion beam and image it to see what it looks like.

PHILOSOPHICAL TRANSACTIONS OF THE ROYAL SOCIETY A MATHEMATICAL, PHYSICAL & ENGINEERING SCIENCES